NIST National Institute of Standards and Technology • U.S. Department of Commerce

Report of Test

Absolute Spectral Radiance Responsivity

of the

NASA GLAMR IGA Radiometer
Model DET-8 IGA, S/N 107

Request Submitted by:

Joel McCorkle
NASA Goddard Space Flight Center
Greenbelt, MD

1. Description of Calibration Items

The device under test (DUT) is an indium gallium arsenide (IGA) radiance meter manufactured by L-1 Standards and Technology, Inc. (L-1), model DET-8 IGA, S/N 107 and referred to as GLAMR IGA in this report. The device is housed in a 2-inch diameter tube with a fore-optic consisting of an aperture and lens. The detector is temperature controlled (L-1 model 3100-1L, S/N 12114) and the rear of the device has inputs for the L-1 temperature controller and a BNC output for the detector signal. The temperature controller was operated with the setpoint at -19.0 °C but only maintained the temperature at -17.547 °C. The detector came with an L-1 model 3300v2, S/N 027, transimpedance amplifier which was used for the calibration. Figure 1.1 shows the detector and accessory equipment as received.

Figure 1.1 Picture of GLAMR IGA Radiometer as received, where it was packaged together with the GLAMR Si Radiometer. The leftmost picture shows the radiometer and the box containing the transimpedance amplifier. Front (center) and back (right) views of the temperature controller are also shown.

1.1 Calibration Request

The request was to calibrate the DUT for absolute radiance responsivity from 885 nm to 1620 nm with a standard uncertainty of 1.7 % (k=1).

2. Description of Test

The detector was characterized for absolute spectral radiance responsivity on the NIST facility for Spectral Irradiance and Radiance responsivity Calibrations using Uniform Sources (SIRCUS).[1,2] The calibration took place in various stages from Aug. 07, 2019 to Aug. 26, 2019. During each calibration test, the detector was temperature controlled with setpoint at -19.0 °C by the L-1 controller but was only maintained at -17.547 °C. The temperature was stable and checked at the beginning and end of each calibration session.

This calibration was performed in two parts. First, the radiance responsivity measured in the spectral range 900 nm to 1655 nm was completed using IGA2017A as the standard reference detector. In the range 1300 nm to 1600 nm, significant errors arose from a two-fold problem. First, the field of view of the DUT requires the source to be placed very close to the detector and the measurement of the source radiance by the reference detector must be done at a much larger distance. Second, errors in the radiance responsivity therefore arise due to differing amounts of atmospheric absorption between the reference detector and DUT with vastly different path lengths. For this reason, an irradiance calibration was also performed in the range 1200 nm to 1655 nm where the measurement could be completed with the source at a fixed Z-position. The irradiance was then scaled by a geometric factor determined as the ratio of irradiance to radiance responsivities in the range 1200 nm to 1300 nm where water absorption was not an issue.

Description of laser systems used: A picosecond mode-locked LBO-OPO laser (~ 80 mHz repetition rate) was used for this calibration. This laser system consists of two different cavities but only the main cavity was used. The main cavity was used in several different ways.

1. The main cavity is designed to oscillate the signal beam and emit it through the output coupler. The output signal beam was used from 900 nm to 1060 nm.
2. When the signal beam is oscillated in the laser cavity, the idler output from the main cavity is ejected from one of the other cavity mirrors. This output of the idler beam was used from 1150 nm to 1655 nm.
3. The main cavity mirrors can also support oscillation of the idler beam when tuned through degeneracy at 1064 nm. In this situation, the idler beam is emitted through the output coupler. The laser was used in this configuration from 1070 nm to 1150 nm.

The output from the lasers was coupled into an optical fiber. The optical fiber was in turn connected to a side port on the integrating sphere and illuminated an area toward the front of the sphere. SIRCUS measurements usually require speckle reduction accomplished by placing the optical fiber in a sonicating bath. For the LBO-OPO system, the bandwidth of the picosecond system is large enough to inherently reduce speckle. A Brokton Electro-Optics Corporation (BEOC) laser power controller stabilized each output beam to less than the 0.1 % level using feedback from a photodiode in the sphere, removing short term as well as long term fluctuations in the power output from the various laser sources. A Bristol 621 wavemeter (S/N: 6208) was used to directly measure the wavelength of the beam oscillated by the main cavity and all wavelengths were converted to the air value for data analysis by dividing by a factor of 1.00027. When the idler beam was used from 1150 nm to 1655 nm, the signal beam was measured by the

wavemeter and converted to the idler wavelength using the relation given by equation 2.1,

$$\lambda_{idler} = \frac{1}{\left(\frac{1}{\lambda_{pump}} - \frac{1}{\lambda_{signal}}\right)} \qquad (2.1)$$

where λ_{pump} is 532.2 nm and λ_{signal} is measured by the Bristol wavemeter.

Integrating Sphere: The integrating sphere used for radiance responsivity was a LabSphere 30.48 cm (12") diameter Spectralon-coated sphere equipped with a 5.08 cm (2") diameter exit aperture fabricated by LabSphere (non-point source geometry).

Data Acquisition and Control Program: The data was acquired using the SIRCUS Main Program v10. Background subtracted DC signals were sequentially collected for each detector (DUT and reference standard) along with simultaneously recorded monitor signals (also background subtracted). The collections were repeated 11 times. Each repeat sample was ratioed to the monitor signal and the average and percent standard deviation was determined.

Description of calibration detectors: The working standard reference detector IGA2017A was used to measure the radiance and irradiance emitted from the source sphere from 900 nm to 1655 nm. It is a single element indium gallium arsenide detector equipped with an aperture having an area of 9.6453 mm^2. IGA2017A was previously calibrated for power responsivity on the NIST Spectral Comparator Facility (SCF), see the file "IGA2017A (SIRCUS) Sumry+Uncert 2017-07-11.xlsx" located on the NIST internal network. The aperture was calibrated at the NIST aperture measurement facility in July 2017.

The monitor detector was an IGA detector mounted directly to the source sphere. It was connected to a Stanford Research Systems current preamplifier (Model SR570, S/N: 57687).

3-axis stage: The integrating sphere is mounted on an XYZ translation stage, with the Z-position (along the optical axis) measured with a linear encoder. The X- and Y-axes enable the source to be properly positioned in front of an instrument before it measures the sphere radiance. The Z-position is used to accurately determine the separation between relevant apertures.

Measurement Setup: Detectors used in these experiments were mounted on tip-tilt stages and aligned to the optical axis of the integrating sphere source using a double-headed laser. To align the detectors to the sphere, the double-headed laser was first mounted in-front of the sphere where one end of the laser was previously aligned to the center of the sphere aperture. The other end of the laser was retroreflected from a glass microscope slide on each detector to align to the optical axis. Lastly, the laser was centered on each detector using the 3-axis stage to determine the X,Y position. See Figures 2.1 and 2.2 for photographs of the measurement setup and Figure 2.3 for a photograph of the temperature controller setup.

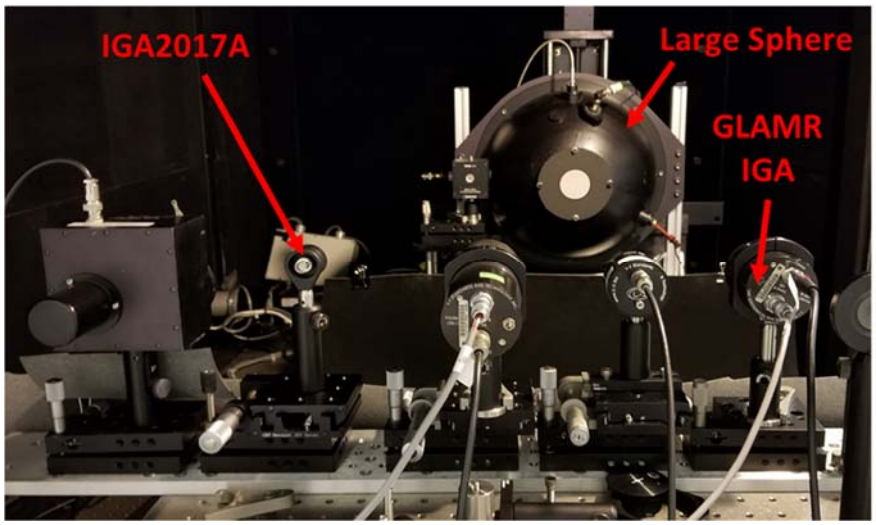

Figure 2.1 Back-view of detector bench setup during the irradiance measurements of the DUT using IGA2017A as the standard reference detectors. It is essentially equivalent to the setup for the radiance measurements except that the 2-inch tube has been removed from the DUT.

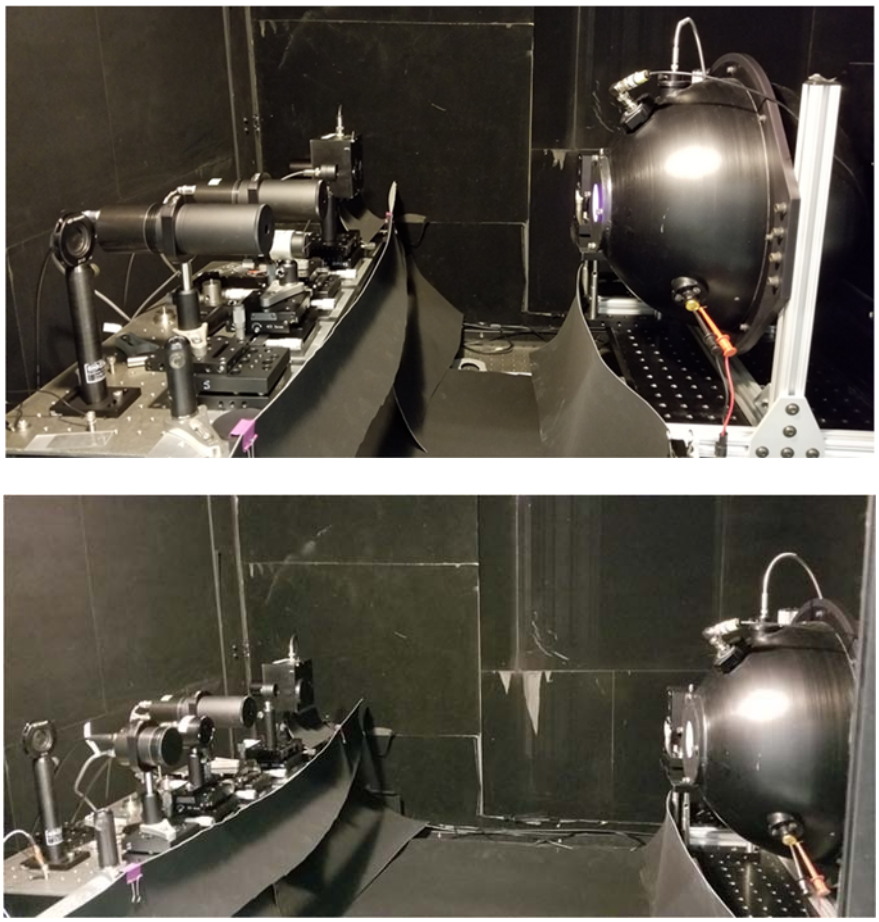

Figure 2.2 Side-views of detector bench setup for radiance (top) and irradiance (bottom) measurements of the DUT using IGA 2017A as the standard reference detectors.

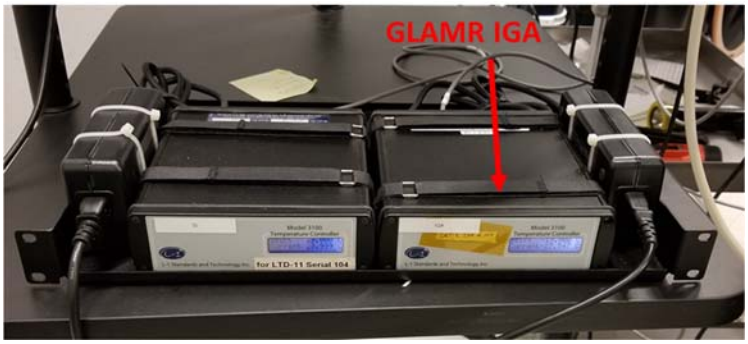

Figure 2.3 Photograph showing the setup of the temperature controllers

2.1 Radiance Responsivity Calibration of GLAMR IGA from IGA2017A

Absolute radiance responsivity measurements for GLAMR IGA (with associated transimpedance amplifier) versus IGA2017A, were completed at discrete wavelengths between 900 nm to 1655 nm using the SIRCUS facility. The integrating sphere source (ISS) was the 12" diameter sphere described in Section 2 with a 5.08 cm (2") aperture. The sphere was moved between different positions for GLAMR IGA and reference standard detector measurements. For GLAMR IGA, a Z-position of -526.55 mm was used. This Z-position was approximately 28 cm away from the front aperture of the DUT, which placed the field of view completely within the 2-inch diameter sphere output aperture. An X-Y response map for the DUT was also measured, verifying the central position and underfilled configuration of the DUT relative to the sphere aperture. The sphere was placed at a different Z-position, -91.823 mm, for measurements of the sphere radiance with IGA2017A. This placed the sphere aperture well within the acceptance angle of the working reference detector for power measurement as suggested in Section 3.1, below. The working distance for IGA2017A was determined from the sphere Z-position and the radiometrically determined detector position, as described in Section 3.2 below.

The pre-amplifier gain was 1 x 10^6 V/A for both detectors for nearly all measurements. The pre-amplifier gain was increased to 1 x 10^7 V/A where the idler power was low at 1150 nm and 1154 nm (case 2 under the laser description section, above).

2.2 Irradiance Responsivity of GLAMR IGA from IGA2017A

Absolute irradiance responsivity measurements for GLAMR IGA (with associated transimpedance amplifier) versus IGA2017A were completed at discrete wavelengths between 1230 nm to 1650 nm using the SIRCUS facility. For these measurements, the 2-inch diameter tube containing the fore-optic was removed, converting the detector to an irradiance meter. The ISS was the 12" diameter sphere described in Section 2 with a 5.08 cm (2") aperture. All measurements were done with the sphere at z = -91.823 mm. The working distance for IGA2017A and GLAMR IGA was determined from the sphere Z-position and the radiometrically determined detector position, as described in Section 3.2 below.

The pre-amplifier gain was 1 x 10^6 V/A for both detectors for all measurements.

2.3 Radiance Responsivity Result of GLAMR IGA from Combined Radiance and Irradiance Measurements

Radiance and irradiance measurements are related by a constant geometric factor equal to the ratio of the two measurements. The two measurements were ratioed between 1230 nm and 1650 nm. Fourteen measurements between 1225 nm and 1340 nm gave a nearly constant ratio where water absorption was not an issue. An average ratio value of 169.32 sr with a percent standard deviation of 0.0118 % resulted. The correction factor was applied to the irradiance data from 1337.6 nm to 1653.6 nm. Overall, the absolute radiance responsivity data therefore consisted of two parts; direct radiance responsivity from 900 nm to 1336 nm and scaled irradiance responsivity from 1337 nm to 1655 mn.

3. Results of Test

For this calibration, both an irradiance and a radiance measurement were performed. In both cases, the reference detector (IGA2017A) establishes the irradiance at the detector aperture plane or the radiance emitted from the source sphere. Even though the reference detectors are irradiance meters, they are also used to determine the source radiance, requiring knowledge of the solid angle of the source. To determine the solid angle, the distance between the trap aperture and the integrating sphere source aperture was measured, along with the integrating sphere and trap aperture areas: See Section 3.1. For the irradiance measurements, the irradiance of the source must be known at the test detector (GLAMR IGA) reference plane. This is done by applying a correction factor to the measured source irradiance at the reference detector reference plane that is derived from the relative positions of the two detectors. The detector positions are determined radiometrically, as described in Section 3.2, and the distance of each from the source is determined by measuring the Z-position with the linear encoder on the Z-axis stage.

3.1 Determination of the sphere source radiance

The radiance of the sphere source was determined with the flux transfer method. A working reference detector (IGA2017A) measured the radiant power from the sphere source passing through two precision apertures, one on the source side, another on the detector side.

The radiance L [W m^{-2} sr^{-1}] of the sphere was determined from radiant power P [W] and the geometric extent G by:

$$L = \frac{P}{G} \tag{3.1}$$

The geometric extent G [m^2 sr] is given by

$$G = \frac{\pi^2}{2}\left[(d^2 + r_s^2 + r_D^2) - \{(d^2 + r_s^2 + r_D^2)^2 - 4r_s^2 r_D^2\}^{1/2}\right] \tag{3.2}$$

where r_S is the radius of the aperture in front of the source, r_D is the radius of the aperture in front of the detector, and d is the distance between the two apertures. The diameter of the sphere aperture was large enough (50.8 mm) to overfill the radiance measurement angle of the DUT radiometer by the sphere output radiation. The distance, d, was chosen large enough (723.69 mm) so that the sphere aperture was well within the acceptance angle of the working reference detector for power measurement.

3.2 Detector offset and offset uncertainty determination for irradiance meters

For both radiance and irradiance measurements, knowledge of a distance between the source and a detector aperture is required. For irradiance measurements, the distance for both IGA2017A (the working reference) and GLAMR IGA (the test detector) was determined. For the radiance measurement, only the distance for the working reference detectors was determined.

All distances were determined radiometrically. In general, at several different Z positions, the detector and monitor voltages were recorded to yield a relative irradiance. Using the $1/Z^2$ law for on-axis irradiance (inverse square law) the resultant data can be fit by a point-source geometry (Equation 3.3) and a non-point-source geometry (the experimental configuration, Equation 3.4) to yield the Z-position of the detector aperture plane. From the Z-position encoder reading used in the radiance and irradiance measurements and the detector Z-position from the radiometric $1/Z^2$ law fit, the actual detector aperture to sphere aperture distance in millimeters (working distance) was determined. Figure 3.1 is a schematic of the configuration.

The inverse square law fitting equation for a point-source geometry is:

$$y = \frac{m_1}{(M_0 - m_2)^2} \tag{3.3}$$

Where y is the relative irradiance, m_1 is a fitting constant, M_0 is Z-position of the integrating sphere that is read by the Z-encoder, and m_2 is the Z-position of zero offset between the two apertures. The fitting uncertainty in m_2, for the sphere position during calibration, gives the uncertainty in the distance between the two apertures.

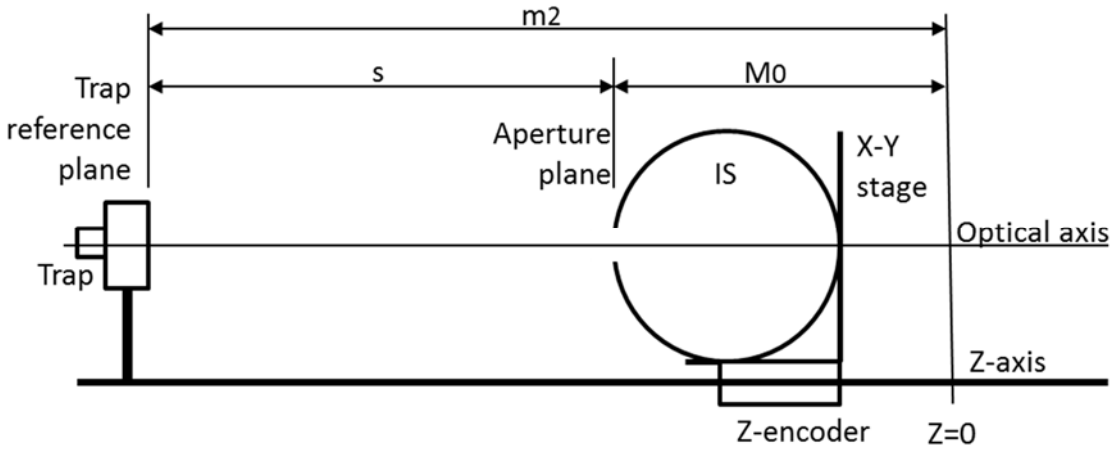

Figure 3.1. Schematic of the configuration for determining trap-sphere distance radiometrically.

If the source aperture is large, the non-point source geometry expression is fit to the data:

$$y = \frac{m_1}{((M_0 - m_2)^2 + m_3^2 + m_4^2)} \tag{3.4}$$

where y, m_1, M_0, and m_2 are the same as in Eq. 3. $m_3 = r_d$, the radius of the detector aperture, and $m_4 = r_s$, the radius of the integrating sphere aperture. Equation 3.4 is valid in the limit where

$$(r_s^2 + r_d^2 + s^2) \gg 2r_s r_d \qquad (3.5)$$

and s is the distance between the source and detector apertures. The inverse square law measurements along with the fit of equation 3.4 to the data for each detector are shown in Figures 3.2 and 3.3, below. At a separation, s, equal to the working distance, the ratio given by equation 3.5 was determined for each detector. This result is summarized in Table 3.1 and shows the condition of equation 3.5 holds and that equation 3.4 is valid in each case. The residuals are approximately 3 orders of magnitude smaller than the base measurement and show there is no obvious bias or offset. The fitting results are also summarized in Table 3.2.

For irradiance measurements, a correction factor (CF) in the source irradiance arises due to slight differences in the working distance between the DUT and reference standard detectors. The correction factor is determined according to equation 3.6 and the detector radius, r_d, refers to either the standard reference detector or the DUT.

$$CF = \frac{r_s^2 + r_{d,ref}^2 + s_{ref}^2}{r_s^2 + r_{d,ref}^2 + s_{DUT}^2} \qquad (3.6)$$

Applying this correction factor gives the source irradiance as measured by the reference standard detector at the DUT reference plane.

Table 3.1 Results of Eq. 3.5 at minimum separation distances.

Detector	r_s (cm)	r_d (cm)	s (cm)	Ratio (Eq 3.5)
IGA2017A	2.54	0.17522	73.0	5994
GLAMR IGA	2.54	0.175	72.5	5919

Table 3.2 Results of the inverse square law fits of equation 3.4 to the data.

Detector	m_2 (mm)	Fitting Uncertainty (mm) (k=1)	R, fit
IGA2017A	-822.35	0.129	1
GLAMR IGA	-817.03	0.228	1

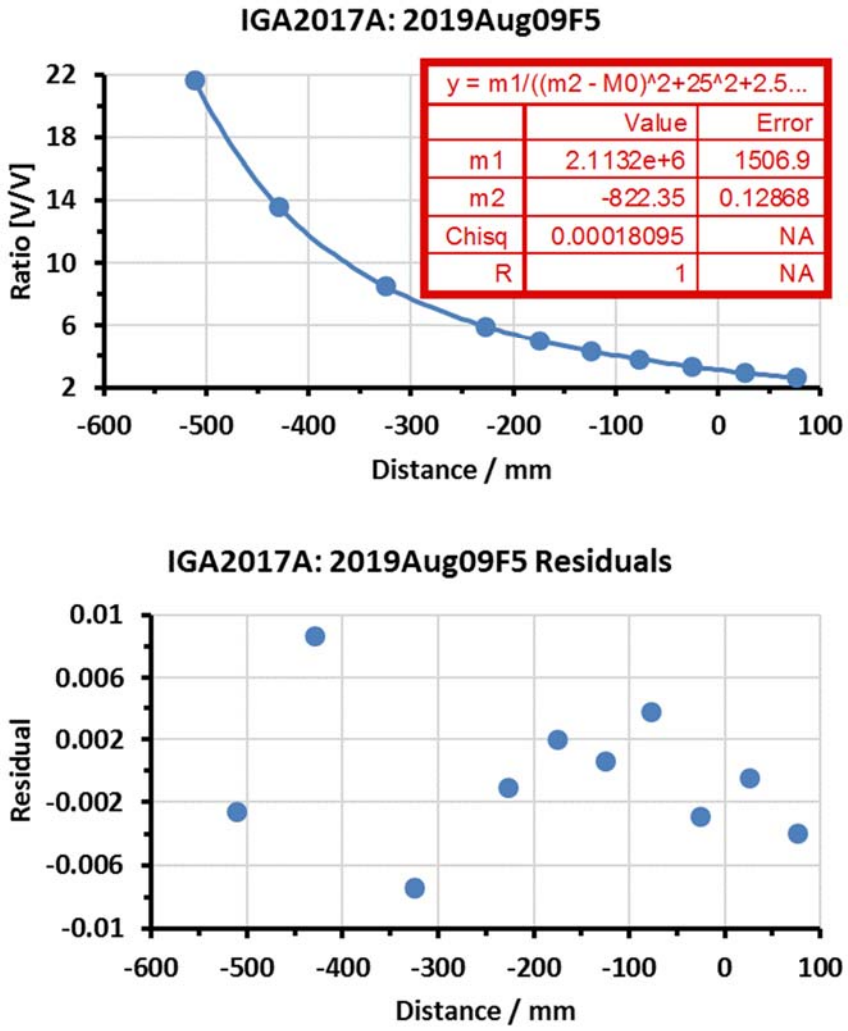

Figure 3.2 Offset and uncertainty fit of the non-point source geometry equation 3.4 to the irradiance response data at a wavelength of 900 nm (top) and residuals from the fit (bottom) for distance determination of IGA2017A for the radiance and irradiance responsivity measurements.

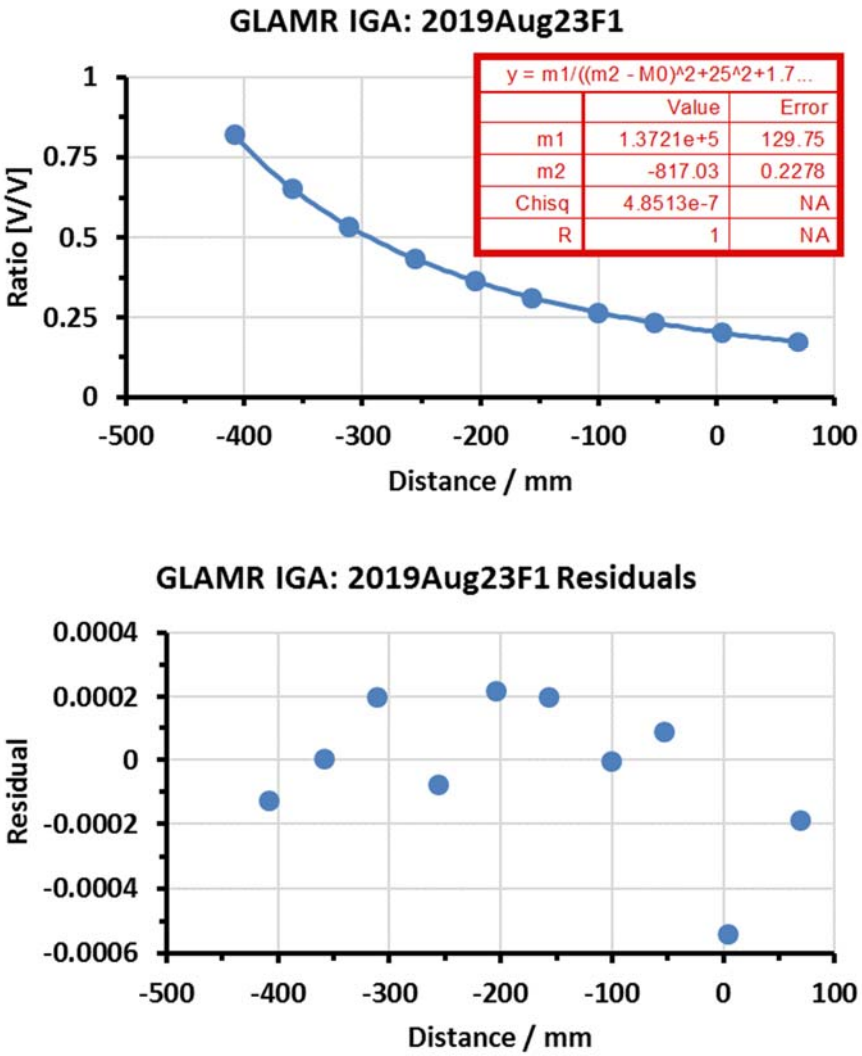

Figure 3.3 Offset and uncertainty fit of the non-point source geometry equation 3.4 to the irradiance response data at a wavelength of 997 nm (top) and residuals from the fit (bottom) for distance determination of GLAMR IGA for the irradiance responsivity measurements.

3.3 Radiance responsivity of GLAMR IGA from IGA2017A

Absolute spectral radiance responsivity of GLAMR IGA was measured from 900 nm to 1655 nm versus IGA2017A. This result is shown in Figure 3.4. Initial analysis of the data revealed unusual fluctuations in the curve between 1300 nm to 1600 nm. These fluctuations were thought to arise due to atmospheric water absorption and differences in the path length between the DUT and reference detector from the source. Therefore, the irradiance responsivity (section 3.4, below) of GLAMR IGA was also measured, where the source could be placed at a fixed Z-position to largely eliminate this path length issue.

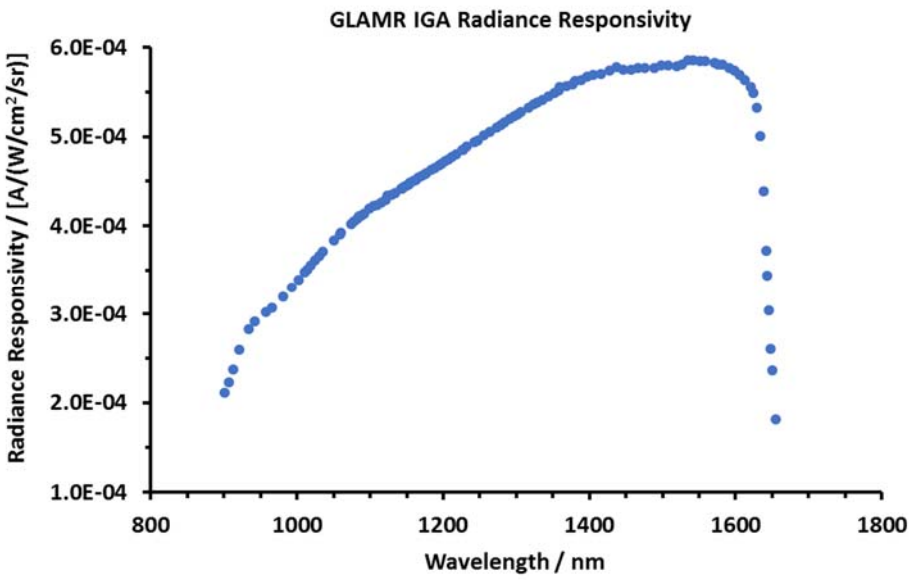

Figure 3.4 Absolute Spectral Radiance Responsivity of GLAMR IGA from IGA2017A as Directly Measured

3.4 Irradiance Responsivity of GLAMR IGA from IGA2017A

Absolute irradiance responsivity of GLAMR IGA from IGA2017A was measured by removing the 2-inch tube containing the fore-optic. This was done to eliminate complications from water absorption where the irradiance responsivity can be measured with the source at a fixed Z-position. This was done from 1225 nm to 1655 nm and is shown in Figure 3.5. The results show that the responsivity curve is much smoother in this region of problematic water absorption.

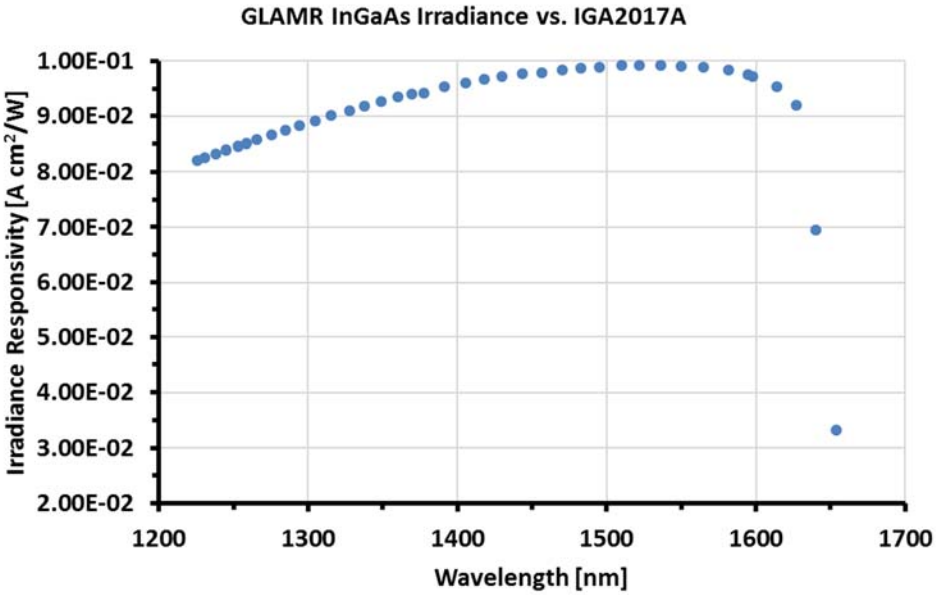

Figure 3.5 Absolute Spectral Irradiance Responsivity of GLAMR IGA from IGA2017A.

3.5 Radiance Responsivity of GLAMR IGA from IGA2017A using Combined Radiance and Irradiance Measurements

The irradiance and radiance results are related by a constant geometric factor given by their ratio. The ratio of those results is shown in Figure 3.6 from 1225 nm to 1655 nm. From 1225 nm to 1130 nm, the ratio of irradiance to radiance is essentially constant with an average value of 169.32 sr with a percent standard deviation of 0.0118 %. The large deviations from this constant value in the remainder of the spectrum arises due to the water absorption present in the radiance measurement. These deviations correspond to an error of about 1.25 % in this spectral region as suggested by the maximum and minimum values of the ratio plot compared to the constant geometric factor found for points less than 1330 nm. Using the geometric factor, the irradiance data was scaled to the radiance data and a comparison of the two results is shown in Figure 3.7. The final data was taken as the direct radiance responsivity from 900 nm to 1336 nm and the scaled irradiance responsivity from 1337 nm to 1655 nm and this data is tabulated in Table 3.3.

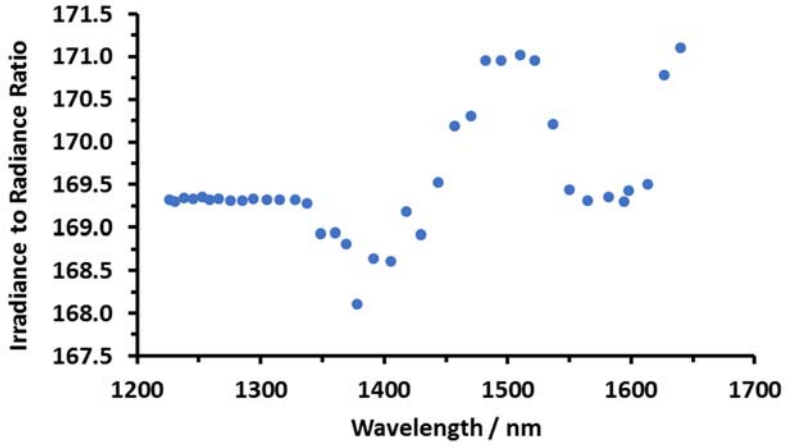

Figure 3.6 Ratio of the irradiance to radiance responsivities of GLAMR IGA from IGA2017A showing the effects of water absorption in the region 1340 nm to 1600 nm.

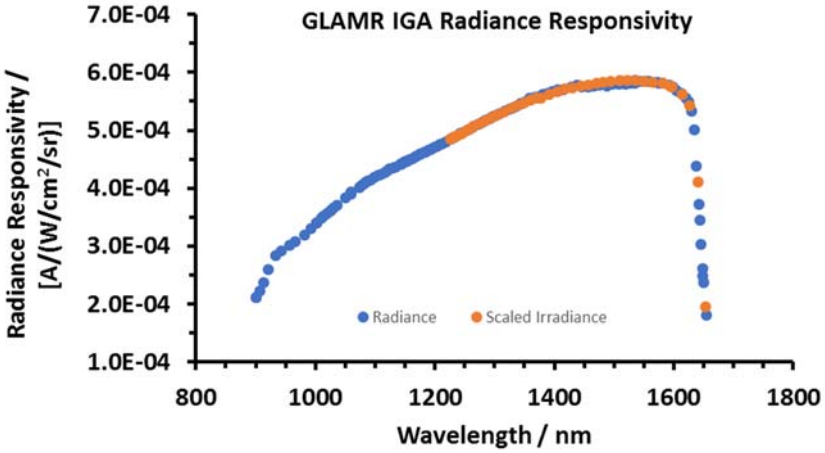

Figure 3.7 Comparison of the direct radiance responsivity to the scaled irradiance responsivity of GLAMR IGA from IGA2017A.

Table 3.3: Tabulated absolute spectral radiance responsivity for GLAMR IGA

Wavelength [nm]	Radiance Responsivity [A/(W/cm²/sr)]	% Uncertainty Total (k=1)
900.39	2.152E-04	0.51
906.79	2.271E-04	0.51
912.79	2.423E-04	0.51
920.57	2.650E-04	0.51
933.25	2.886E-04	0.51
942.45	2.972E-04	0.51
957.09	3.077E-04	0.51
965.51	3.132E-04	0.51
981.00	3.258E-04	0.51
992.63	3.367E-04	0.51
1001.84	3.459E-04	0.51
1010.27	3.543E-04	0.51
1013.53	3.574E-04	0.51
1018.82	3.626E-04	0.51
1024.68	3.681E-04	0.51
1030.08	3.731E-04	0.51
1035.49	3.780E-04	0.51
1050.78	3.912E-04	0.51
1058.83	3.978E-04	0.51
1060.25	3.998E-04	0.51
1073.81	4.095E-04	0.51
1077.44	4.122E-04	0.51
1081.82	4.159E-04	0.51
1084.75	4.182E-04	0.51
1087.71	4.195E-04	0.51
1092.17	4.215E-04	0.51
1099.01	4.271E-04	0.51
1104.32	4.300E-04	0.51
1109.64	4.312E-04	0.51
1115.03	4.343E-04	0.51
1120.57	4.374E-04	0.51
1123.70	4.416E-04	0.51
1129.28	4.435E-04	0.51
1134.10	4.455E-04	0.51
1142.14	4.504E-04	0.51
1145.39	4.515E-04	0.51
1148.67	4.526E-04	0.51
1150.04	4.541E-04	0.52

1152.72	4.554E-04	0.51
1154.31	4.565E-04	0.51
1158.47	4.584E-04	0.51
1161.94	4.596E-04	0.51
1166.27	4.624E-04	0.51
1170.73	4.647E-04	0.51
1175.17	4.670E-04	0.51
1176.90	4.678E-04	0.51
1183.55	4.712E-04	0.51
1188.57	4.740E-04	0.51
1193.78	4.767E-04	0.51
1197.75	4.789E-04	0.51
1202.78	4.814E-04	0.51
1207.27	4.839E-04	0.51
1211.71	4.863E-04	0.51
1217.69	4.896E-04	0.51
1225.95	4.942E-04	0.51
1226.60	4.945E-04	0.51
1232.34	4.978E-04	0.51
1242.57	5.033E-04	0.51
1246.84	5.056E-04	0.51
1255.99	5.108E-04	0.51
1264.27	5.154E-04	0.51
1272.85	5.201E-04	0.51
1278.74	5.233E-04	0.51
1284.11	5.262E-04	0.51
1291.36	5.300E-04	0.51
1296.57	5.326E-04	0.51
1300.90	5.348E-04	0.51
1306.68	5.378E-04	0.51
1316.32	5.425E-04	0.51
1323.69	5.461E-04	0.51
1328.76	5.485E-04	0.51
1336.02	5.517E-04	0.51
1337.60	5.525E-04	1.35
1348.86	5.572E-04	1.35
1360.32	5.625E-04	1.35
1369.62	5.657E-04	1.35
1377.82	5.668E-04	1.49
1390.97	5.734E-04	1.35
1405.63	5.781E-04	1.35
1418.09	5.818E-04	1.35
1429.49	5.846E-04	1.35

1443.64	5.876E-04	1.35
1456.77	5.893E-04	1.35
1470.12	5.916E-04	1.35
1482.36	5.936E-04	1.35
1494.79	5.954E-04	1.35
1510.30	5.966E-04	1.35
1521.76	5.969E-04	1.35
1536.35	5.968E-04	1.35
1549.70	5.964E-04	1.35
1564.83	5.948E-04	1.35
1581.84	5.917E-04	1.35
1594.42	5.869E-04	1.35
1597.61	5.854E-04	1.35
1613.64	5.735E-04	1.35
1626.77	5.536E-04	1.37
1640.02	4.186E-04	1.38
1653.56	1.996E-04	1.63

Section 3.6 Uncertainty Analysis for the Radiance Responsivity of GLAMR IGA

Table 3.3 Uncertainty Budget for Absolute Spectral Radiance Responsivity of GLAMR IGA.

	Relative Standard Uncertainty [%]	
Uncertainty Component	**Radiance 900 nm to 1336 nm**	**Scaled Irradiance 1337 nm to 1655 nm**
Measurement % Standard Deviation[1]	0.02	0.03
Reference detector Irrad. Cal. (IGA2017A from SCF; July 2017)	0.4	0.4
Reference Detector Uniformity	0.3	0.3
Reference Detector Distance	0.02	0.02
DUT Distance	N.A.	0.03
Amplifier gain	0.05	0.05
Geometry Alignment	0.05	0.05
Reference Detector Aperture Area	0.03	0.03

Sphere Aperture Area	0.03	0.03
Wavelength	0.01	0.01
Irradiance Scaling Factor[2]	N.A.	0.012
Water Absorbance[3]	N.A.	1.25
Combined Standard Uncertainty (k=1)	**0.51**	**1.35**

Note 1: This is the average measurement percent standard deviation across the entire range. Value for individual wavelengths are provided in the calibration file.
Note 2: This is the average of the irradiance to radiance ratio in the range 1230 nm to 1330 nm.
Note 3: Errors induced by water absorption in the radiance measurement are based on the difference between the direct radiance and average value of the irradiance/radiance ratio where water absorption is not problematic (1230 nm to 1330 nm). 1.25 % is essentially the amount by which the radiance data is scaled in the region 1330 nm to 1650 nm.
Note 4: This is not the full calibration uncertainty budget. The uncertainty budget, Table 3.4, does not include environmental effects on both the reference detector and the GLAMR radiometer. No evaluations of instrument performance characteristics such as temperature dependence, response linearity or temporal stability were performed. For estimates in the interpolated uncertainty, see the reference.[3]

4. General Information

It should be noted that the reported results were derived from using the dial gain value on the provided pre-amplifiers (i.e. 1 x 10^6 V/A) to give the radiance responsivity in [A/(W/cm^2/sr)]. This assumes that the transimpedance amplifier for each DUT has been calibrated and the dial gain values have high accuracy (to say 0.05 % or better). If this is not the case, we need either to obtain the gain correction factors for those pre-amplifiers or can only report the calibration for each device as a whole system (i.e. detector plus pre-amplifier) in units of [V/(W/cm^2/sr)] for radiance.

Information was recorded in the SIRCUS Vis #20 laboratory notebook, pp.105-121.

The calibration measurements were performed by Brian Alberding and John Woodward. The data analysis and report writing was performed by Brian Alberding.

This calibration required 10 days of laboratory work (including setup, troubleshooting, and data collection) on SIRCUS and 7 days of data reduction, analysis, and reporting.

Significant experimental notes:

1. There was a mistake in the radiance responsivity analysis where the incorrect IGA2017A position was used. This was noticed and corrected on 11/21/19 during report writing and affects the values originally delivered to NASA on 10/30/19.

Information about data files:

1. Full data files for the radiance responsivity of GLAMR Si are located on Elwood under:

   \\cfs2e.nist.gov\685\internal\G04\Sircus\SIRCUS\Calibrations\SIRCUS Calibrations\FY 2019 Calibrations\GLAMR\GLAMR InGaAs

Data file for the radiance responsivity of GLAMR IGA: "Combined Irradiance and Radiance Responsivity GLAMR InGaAs from IGA2017A.xlsx"

The files located in these directories are meant for internal NIST use only. Please do not distribute without authorization.

References

1. Brown, S. W., Eppeldauer, G. P. & Lykke, K. R. Facility for spectral irradiance and radiance responsivity calibrations using uniform sources. *Appl. Opt., AO* **45**, 8218–8237 (2006).
2. Woodward, J. T. *et al.* Invited Article: Advances in tunable laser-based radiometric calibration applications at the National Institute of Standards and Technology, USA. *Review of Scientific Instruments* **89**, 091301 (2018).
3. Gardner, J. L. Uncertainties in Interpolated Spectral Data. *J. Res. Natl. Inst. Stand. Technol.* **108**, 69–78 (2003).

Distribution Restrictions: None

Tabulated calibration data files were provided along with this report.
Filename: "GLAMR InGaAs Calibration Aug 2019_Data Delivered to NASA.xlsx"

Prepared by:

Brian G. Alberding
Remote Sensing Group
Sensor Science Division
Physical Measurement Laboratory
(301) 975-4664

Approved by:

Joseph P. Rice, Leader
Remote Sensing Group
Sensor Science Division
Physical Measurement Laboratory
(301) 975-2133